

Research Report

Preliminary Orbital Elements Determination of Asteroids Using the Gauss Method

Sebastián Hermosilla^{1,2}

1. Faculty of Physical and Mathematical Sciences, University of Chile, Beaucheff 850, Santiago de Chile

2. Astronomy department, University of Chile, Camino El Observatorio 1515, Las Condes

e-mail: s.hermosilla@ing.uchile.cl

June, 2023

ABSTRACT

Orbit determination plays an important role in the characterization of asteroids. Among the methods available, this report delves into the Gauss method, Investigating both its accuracy and inherent limitations. The mathematical underpinnings of the method are discussed, followed by a practical implementation in Python and a series of tests to evaluate its performance. The Gauss method's susceptibility to the time intervals between observations is studied, shedding light on the optimal conditions for its application. Noteworthy outcomes encompass the successful determination of Ceres and 2002 KM6's orbits. Additionally, upper and lower thresholds for the time intervals during Ceres' observations are uncovered (~ 1 day - ~ 250 days), contributing to the understanding of the method's sensitivity.

1. Introduction

Asteroids, rocky remnants of the early solar system, are crucial for understanding its formation and evolution. Studying these minor planets provides insights into the conditions that shaped our cosmic environment.

In addition to their historical significance, asteroids pose potential risks to Earth. Impacts can cause significant damage and harm human lives. For example, the Chelyabinsk meteor's impact in Russia in 2013 underscored the need to detect Near Earth Asteroids (NEAs) and develop planetary defense strategies.

Determining the orbits of asteroids is essential for planetary defense and understanding their formation. Precise orbit calculations reveal valuable information about their family relationships and history. By tracking their positions and movements, we gain deeper insights into their shape, rotation, and the dynamic processes that contributed to the formation of our solar system.

Moreover, determining the orbits of asteroids can significantly facilitate future space missions. Precisely known orbits enable spacecraft to approach these celestial bodies efficiently. As a result, orbital determination plays a crucial role in the field of planetary science and asteroid monitoring.

This report introduces the Gauss method implementation, an algorithm for preliminary orbit determination. Developed by Carl Friedrich Gauss, this method aimed to predict the position of Ceres, the first discovered asteroid. After Giuseppe Piazzi's sighting of Ceres in January and February 1801, the asteroid was lost due to the Sun's glare, making tracking and recovery impossible. In response, Gauss devised his method, offering a solution to estimate the orbit within limited observation intervals.

Determining the orbital elements of an asteroid only requires obtaining its position and velocity data at a specific moment. Subsequently, the problem can be simplified by using a series of observational coordinates to calculate the position and velocity at any given observation.

In this text, my aim is to thoroughly explain the algorithm and back it up with orbit predictions. Afterward, I will move on to comparing and analyzing the results. Additionally, I'll explore how the method behaves with different initial conditions to understand the appropriate scenarios for its utilization.

2. Gauss Method

Determining an orbit involves defining six distinct parameters, which can either be the orbital elements or the three components of the position and velocity vector.

To establish the orbit based solely on observations, six independent measurements are required. The Gauss method employs the right ascension (α) and declination (δ) of each observation to calculate the asteroid's position and velocity. This necessitates three separate images to accomplish orbit determination.

The vector being sought through the algorithm directs from the Sun to the asteroid and is represented as \mathbf{r} in Figure 1. This vector can be computed in a more straightforward manner by treating it as the sum of the vector from the Sun to Earth (\mathbf{R}) and the vector from Earth to the asteroid (ρ).

$$\mathbf{r} = \mathbf{R} + \rho$$

This is owing to the fact that the value of \mathbf{R} is established, and the orientation of ρ is determined by the observation's co-

ordinates. It is noteworthy that for this assertion to hold true, it is imperative to operate within an equatorial-aligned reference frame. Without such alignment, the straightforward transformation of declination and right ascension into the directional vector from Earth to the asteroid cannot be achieved.

Keeping this in consideration, we can formulate the vector for each of the observations as follows:

$$\mathbf{r}_i = \mathbf{R}_i + \|\rho_i\|\hat{\rho}_i; \quad i = 1, 2, 3 \quad (1)$$

For the i -th observation, $\hat{\rho}_i$ is defined as:

$$\hat{\rho}_i = (\cos \alpha_i \cos \delta_i, \sin \alpha_i \cos \delta_i, \sin \delta_i)$$

Due to the Keplerian nature of the orbit, all vectors originating from the Sun and pointing to the asteroid should lie within the same plane. Consequently, the vectors $\mathbf{r}_1, \mathbf{r}_2, \mathbf{r}_3$ are expected to exhibit linear dependence:

$$c_1 \mathbf{r}_1 + c_2 \mathbf{r}_2 + c_3 \mathbf{r}_3 = 0$$

Without loss of generality, it is feasible to set $c_2 = -1$, leaving the other constant to be determined:

$$c_1 \mathbf{r}_1 + c_3 \mathbf{r}_3 = \mathbf{r}_2 \quad (2)$$

If we consider that the observation were taken close enough, we can express the position vector \mathbf{r}_i as an expansion of the vector \mathbf{r}_2 :

$$\mathbf{r}_i = \mathbf{r}_2 + \dot{\mathbf{r}}_2 \Delta t_i + \frac{1}{2} \ddot{\mathbf{r}}_2 \Delta t_i^2 + \frac{1}{6} \ddot{\mathbf{r}}_2 \Delta t_i^3 + O(\Delta t_i^4)$$

Here, Δt_i denotes the time span between observations.

Applying the potential of the two-body problem, we can substitute the values of the higher-order derivatives ($\ddot{\mathbf{r}}_2$ and $\ddot{\mathbf{r}}_2$) as follows:

$$\ddot{\mathbf{r}}_2 = \frac{-\mu \mathbf{r}_2}{\|\mathbf{r}_2\|^3}$$

Here, μ represents the gravitational parameter of the Sun.

Subsequently, if we introduce the definitions:

$$f_i = 1 - \frac{1}{2} \frac{\mu \Delta t_i^2}{\|\mathbf{r}_2\|^3} \quad g_i = \Delta t_i - \frac{1}{6} \frac{\mu \Delta t_i^3}{\|\mathbf{r}_2\|^3}$$

The expansion of \mathbf{r}_i in terms of \mathbf{r}_2 takes the form:

$$\mathbf{r}_i = f_i \mathbf{r}_2 + g_i \ddot{\mathbf{r}}_2$$

By substituting the approximations of \mathbf{r}_1 and \mathbf{r}_3 into equation (2), the constants can be determined, yielding:

$$c_1 = \frac{g_3}{f_1 g_3 - f_3 g_1} \quad c_3 = \frac{g_1}{f_1 g_3 - f_3 g_1}$$

Thus, the values of c_1 and c_3 are contingent solely on $\|\mathbf{r}_2\|$.

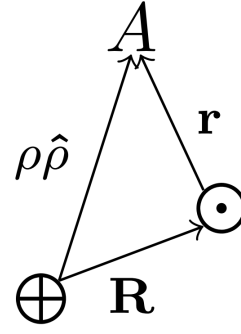


Fig. 1. The diagram depicts vectors used in the Gauss Method for orbital determination of asteroids. \mathbf{r} represents the Sun-to-Asteroid direction. \mathbf{R} points from the Sun to Earth. $\rho\hat{\rho}$ indicates the Earth-to-Asteroid vector (distance and direction). Accurate calculations of these vectors are crucial for determining orbital elements and predicting asteroid positions.

Substituting equation (1) into (2) allows us to eliminate $\mathbf{r}_1, \mathbf{r}_2$, and \mathbf{r}_3 , resulting in the following relation:

$$c_1(\mathbf{R}_1 + \|\rho_1\|\hat{\rho}_1) + c_3(\mathbf{R}_3 + \|\rho_3\|\hat{\rho}_3) = \mathbf{R}_2 + \|\rho_2\|\hat{\rho}_2$$

It's noteworthy that this relationship furnishes three equations with four unknowns ($\|\rho_1\|, \|\rho_2\|, \|\rho_3\|$, and $\|\mathbf{r}_2\|$).

The ultimate equation for the problem is obtained by taking the dot product of equation (1) with itself during the time of the second observation:

$$\mathbf{r}_2 \cdot \mathbf{r}_2 = (\mathbf{R}_2 + \|\rho_2\|\hat{\rho}_2) \cdot (\mathbf{R}_2 + \|\rho_2\|\hat{\rho}_2)$$

$$\|\mathbf{r}_2\|^2 = \|\mathbf{R}_2\|^2 + 2\|\rho_2\|(\hat{\rho}_2 \cdot \mathbf{R}_2) + \|\rho_2\|^2 \quad (3)$$

By rearranging the terms in these four equations, we arrive at the following equation for $\|\mathbf{r}_2\|$:

$$\|\mathbf{r}_2\|^8 - (A^2 + 2A \langle \rho_2, \mathbf{R}_2 \rangle + \|\mathbf{R}_2\|^2) \|\mathbf{r}_2\|^6 - 2B(A + \langle \rho_2, \mathbf{R}_2 \rangle) \|\mathbf{r}_2\|^3 - B^2 = 0$$

This equation takes the form of an 8th-degree polynomial. Consequently, the utilization of a numerical method is imperative to ascertain the solutions. Disregarding the negative and imaginary roots is essential. In instances where multiple positive solutions exist, all of them should be regarded as potential solutions.

After finding the value of $\|\mathbf{r}_2\|$, we can determine $\|\rho_1\|, \|\rho_2\|$, and $\|\rho_3\|$. Using equation (1), we can then compute the vectors $\mathbf{r}_1, \mathbf{r}_2$, and \mathbf{r}_3 . Finally, we can calculate the value of $\ddot{\mathbf{r}}_2$ by reversing the expansion of \mathbf{r}_i :

$$\ddot{\mathbf{r}}_2 = \frac{\mathbf{r}_i}{g_i} - \frac{f_i}{g_i} \mathbf{r}_2$$

Following this procedure, the values of \mathbf{r}_2 and $\ddot{\mathbf{r}}_2$ are calculated, marking the completion of the method. For a more comprehensive explanation, please consult references [3], [4], and [6] in the bibliography.

Upon estimating the orbit, an iterative technique is applied to the outcome, utilizing differential corrections to enhance the predictions. A comprehensive guide on this process can be found in the book "Orbital Mechanics for Engineering Students," included in the bibliography (p242, p243) [4].

3. Implementation and Testing

The implementation of the Gauss Method follows the procedure outlined in [4] and incorporates some functions from GitHub repositories [7] and [8] from the bibliography. The algorithm relies on input vectors \mathbf{R} , sourced from NASA's JPL Horizons System, representing the vector from the Sun to Earth for each observation.

3.1. Testing with Horizons

To assess the algorithm's functionality, I will apply it to determine the orbital elements of Ceres. For this purpose, I will collect the Right Ascension and Declination values of the asteroid at three distinct time points. Table 1 presents the coordinates of Ceres and the selected moments for the orbit determination.

Executing the algorithm with these observations yields the outcomes presented in Table 2. The table also displays the discrepancies between each of the osculating orbital elements and the values provided by the Horizons System.

Most of the orbital elements show slight variations, except for the Argument of Perifocus (w), which exhibits a substantial error of 125%. One plausible explanation for this disparity could be that the algorithm encounters difficulty in accurately determining the Perifocus of an orbit that is nearly circular.

3.2. Testing with Real Observations.

After confirming the algorithm's functionality, the subsequent step involved utilizing actual observations to deduce an asteroid's orbit. For this purpose, I employed observations presented in the paper "Orbit determination of Asteroid 2002 KM6" authored by Lee, Lu, and Moyer, published in 2019 [5]. In this publication, the authors furnish the asteroid's coordinates derived from an observation campaign, along with the associated observation errors. Employing this data, I performed a Gaussian perturbation of the observations, using the reported error as the standard deviation. Table 3 showcases the celestial coordinates of the observations, their respective errors, and the corresponding timestamps.

$$\delta_{used} = \delta_{obs} + N(0, \delta_{error})$$

$$\alpha_{used} = \alpha_{obs} + N(0, \alpha_{error})$$

Employing the implemented Gauss Method with the perturbed coordinates enables the establishment of a confidence interval for the orbital parameters. Figure 2 illustrates the orbital element estimations for the Asteroid 2002 KM6. The figure showcases a perturbation of 10000 in the observation coordinates. Furthermore, it displays both the median value with the one-sigma error range for each orbital element, and the corresponding value from the Horizons system for the asteroid at that precise instance.

Notably, as all the Horizons values lie within the 1-sigma error range offered by the algorithm, and considering the relatively minor magnitude of these errors, it becomes apparent that the algorithm adeptly fulfills the mission of determining the asteroid's orbit.

Figure 3 illustrates the orbit prediction for the same asteroid, but with the selection of an alternative root of the 8-degree polynomial. The visual representation highlights that opting for the incorrect solution of the polynomial can lead the algorithm to converge toward entirely erroneous values.

Time	RA	DEC
2023-07-02T06:53:11.616	185.899	7.188
2023-07-26T06:53:11.616	192.899	2.835
2023-08-20T06:53:11.616	200.079	-1.819

Table 1. Dates employed in the orbit estimation of Ceres. The Right Ascension and Declination values from Horizons are presented in degrees.

Orbital Elements	Calculated	Horizons	Error
Semi-Major Axis [AU]	2.80	2.76	1.50%
Eccentricity	0.08	0.08	0.00%
Inclination (°)	27.20	27.19	0.03%
Longitude of A. Node (°)	23.28	23.35	0.30%
Argument of Perifocus (°)	298.35	132.53	125.12%
Mean Anomaly (°)	44.86	49.63	9.61%

Table 2. Osculating orbital elements computed for the orbit of Ceres, along with the corresponding values provided by Horizons. The last column illustrates the discrepancy between the predictions and the Horizons values.

3.3. Using Tycho for a complete process of detection and orbit determination of an asteroid

Upon successfully determining the orbit using the algorithm, it becomes essential to understand how to utilize an Asteroid detection software to oversee the complete process of detecting and characterizing an Asteroid.

Tycho is a software designed to facilitate various tasks related to Asteroid detection (Daniel Parrot, 2020 [2]). With Tycho, you can seamlessly upload your observations and conduct tasks like calibration, alignment, and plate solving of images. After image processing, the software's detection algorithm can be employed to identify any moving object. Tycho then generates a list of all detected asteroids for your reference.

To initiate the process, the software provides a selection of image sets. I chose a set comprising 60 images and executed the detection algorithm. Among the various asteroids identified, I focused on the brightest detection to facilitate orbit determination. This specific detection corresponded to the Asteroid 2000 RZ92.

Tycho provides the observation coordinates for further analysis. These values were used for determining the asteroid's orbit. The observations lack associated errors. As a workaround, I adopted the pixel size multiplied by the number of pixels that detect the asteroid as an approximation for the observation error.

To take advantage of the multitude of available images, I opted to select ten groups of three images each. Subsequently, I determined the orbit for each trio individually. The collective predictions from all these analyses were then amalgamated to derive the final parameters. The outcomes are showcased in Figure

Observations	RA	DEC	Time
Obs 1	264.496 \pm 0.00345	-24.906182 \pm 0.0005	2019-07-07T06:40:19.200
Obs 2	264.639 \pm 0.00345	-22.779707 \pm 0.0005	2019-07-15T06:31:40.800
Obs 3	264.926 \pm 0.00345	-21.790782 \pm 0.0005	2019-07-19T06:34:33.600

Table 3. Observations extracted from the paper "Orbit determination of Asteroid 2002 KM6". These observations served as a test for the algorithm using real data. The table presents the dates of the three observations and the associated error in the celestial coordinates.

Orbital elements estimation for Asteroid 2002 KM6

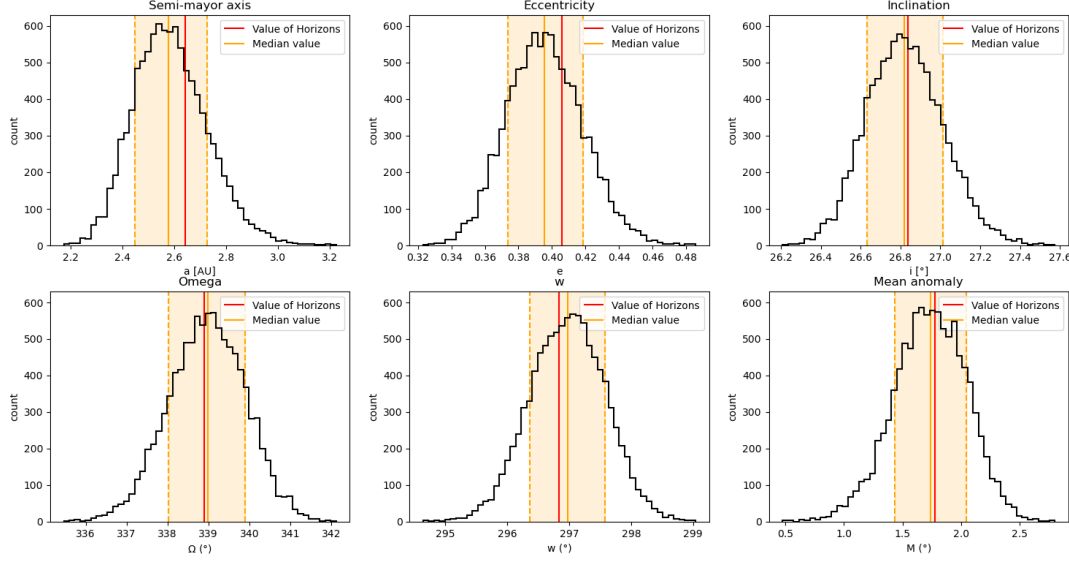


Fig. 2. Orbit determination based on actual observations. The yellow lines represent calculations made using the algorithm, with the shaded area indicating the 1-sigma error associated with these predictions. Conversely, the red line depicts the value provided by Horizons.

4. The plot visually conveys that the orbit predictions exhibit noticeable inaccuracies. This could potentially be attributed to the relatively short time intervals between observations, approximately 20 minutes.

4. Accuracy of the algorithm as a function of time in between the observations

In a final exploration of the Gauss method, I aimed to investigate how the algorithm's error behaves with an increasing time interval between observations.

For this, I used the Horizons System to obtain three observations of Ceres separated by one day. Then I repeat the process increasing the time in between the observation every time more until I reach 1 year of separation in between the observations.

To explore shorter time intervals, the process is replicated by commencing with images spaced 1 minute apart and progressively increasing the time gap until a full day is achieved.

The findings of this investigation are showcased in Figures 5 and 6. The plot illustrating extended time-intervals between observations (fig 5) presents reliable predictions of the osculating orbital elements until a time gap of around ~ 250 days is encountered. Conversely, when considering shorter observation time spans (fig 6), the results exhibit an enhancement as they approach the one-day separation mark. This insight provides sup-

port for explaining why the orbit determination for 2000 RZ92, detected with Tycho, encountered challenges.

5. Conclusions

In conclusion, the implementation of the Gauss method for orbital determination presents valuable insights into its efficacy and limitations. The analysis undertaken underscores the method's potential as a reliable tool for obtaining initial estimates of orbital elements.

However, it is essential to acknowledge the method's inherent constraints. The Gauss method exhibits susceptibility to varying time intervals between observations, which can impact the accuracy of predictions. Moreover, the requirement to solve high-degree polynomials introduces complexity and the possibility of multiple solutions.

The findings highlight the importance of strategic algorithm selection in orbit determination endeavors. Integrating the strengths of the Gauss method alongside other techniques can potentially mitigate its limitations, leading to more precise and comprehensive orbit determinations.

In summary, the Gauss method serves as a promising initial step in the process of orbital determination. By leveraging its benefits in tandem with other techniques, the overall accuracy and reliability of orbit determination can be significantly enhanced.

Orbital elements estimation for Asteroid 2002 KM6

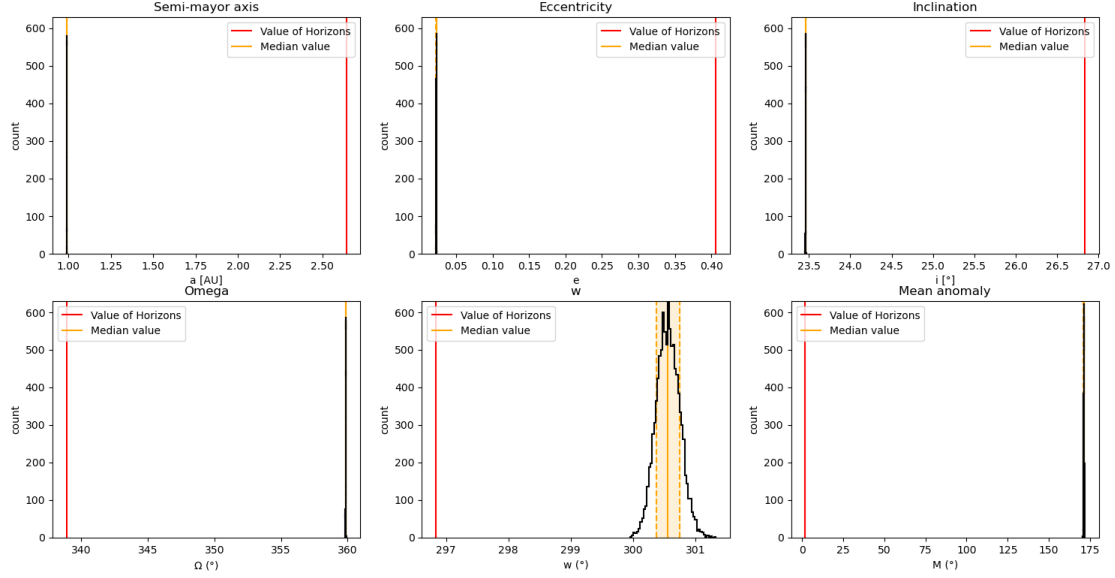


Fig. 3. Orbit determination based on real observations, with the selection of an incorrect polynomial solution. The yellow lines depict calculations using the algorithm, while the shaded area represents the 1-sigma error associated with these predictions. In contrast, the red line corresponds to the value provided by Horizons.

6. Bibliography

- [1] CHUNYANG DING, HANNAH NIKOLE ALMONTE, AND JOAN CREUS COSTA, 2014 *Orbit Determination for Asteroid 214088 (2004 JN13) Using Gauss' Method*
- [2] DANIEL PARROT; 2020
Tycho Tracker: A New Tool to Facilitate the Discovery and Recovery of Asteroids Using Synthetic Tracking and Modern GPU Hardware
- [3] GIOVANNI F. GRONCHI, 2004 *Classical and modern orbit determination for asteroids*
- [4] HOWARD CURTIS; 2023
Orbital Mechanics for Engineering Students
- [5] HYUNJIN LEE, CATHERINE LU, CARTER MOYER, 2019
Orbit determination of asteroid 2002 KM6
- [6] VERNET, J; 2011
A COMPREHENSIVE COMPARISON BETWEEN ANGLES-ONLY INITIAL ORBIT DETERMINATION TECHNIQUES
- [7] ORBITDETERMINATION; 2012
<https://github.com/JhonCory/OrbitDetermination.git>
- [8] ORBITDETERMINATOR; 2017
<https://github.com/aerospaceresearch/orbitdeterminator.git>

Orbital elements estimation

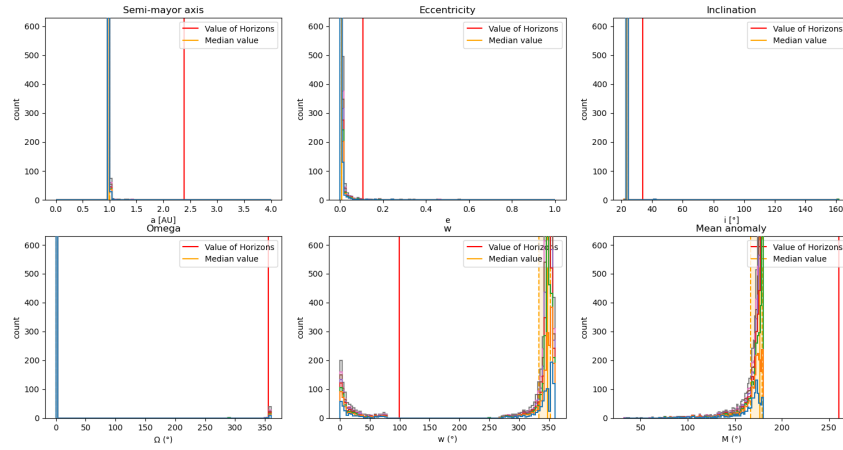


Fig. 4. Orbit determination of the asteroid identified using the Tycho software. Distinctly colored histograms signify diverse orbit estimations derived from varying sets of image trios, overlaid on top of each other. The red line represents the value supplied by Horizons for the same asteroid.

Error in the estimated orbital elements as a function of time

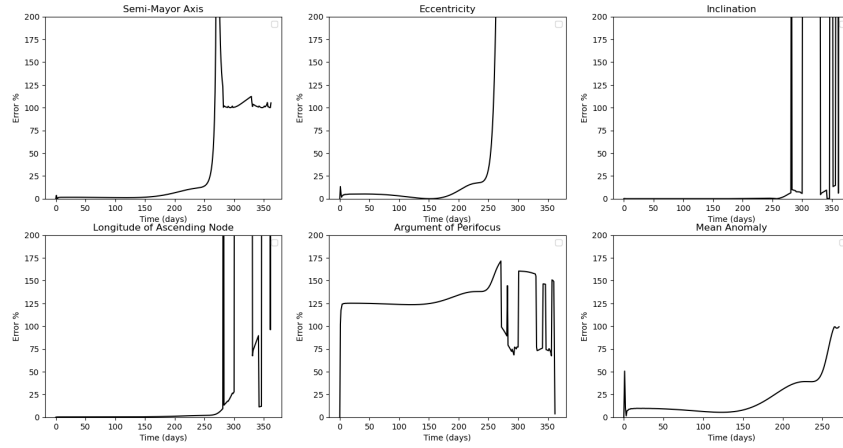


Fig. 5. Error in the orbital parameters estimated with the algorithm as a function of time.

Error in the estimated orbital elements as a function of time

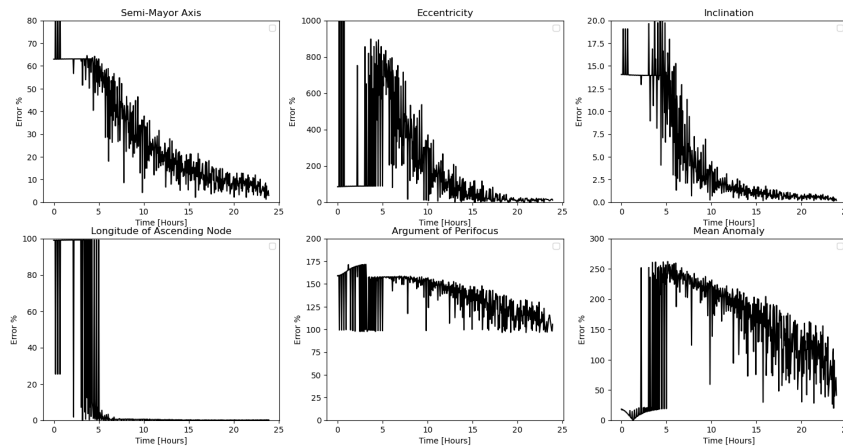


Fig. 6. Error in the orbital parameters estimated with the algorithm as a function of time.